

Exact Kalman Filter for Binary Time Series

Augusto Fasano, Giovanni Rebaudo, Daniele Durante and Sonia Petrone

Bocconi University, Department of Decision Sciences, Via Röntgen 1, 20136, Milan, Italy

Summary. Non-Gaussian state-space models arise routinely in several applications. Within this framework, the binary time series setting provides a source of constant interest due to its relevance in a variety of studies. However, unlike Gaussian state-space models—where filtering and predictive distributions are available in closed form—binary state-space models require either approximations or sequential Monte Carlo strategies for inference and prediction. This is due to the apparent absence of conjugacy between the Gaussian states and the probit or logistic likelihood induced by the observation equation for the binary data. In this article we prove that the filtering and predictive distributions of dynamic probit models with Gaussian state variables belong to the class of unified skew-normals (SUN) and the associated parameters can be updated recursively via analytical expressions. Also the functionals of these filtering and predictive distributions depend on known functions, but their calculation requires Monte Carlo integration. Leveraging the SUN results, we address this point by proposing methods to draw independent and identically distributed samples from filtering and predictive distributions, thereby improving state-of-the-art approximate or sequential Monte Carlo inference in small-to-moderate dimensional dynamic models. A scalable and optimal particle filter which exploits SUN properties is also developed and additional exact expressions for the smoothing distribution are provided.

Keywords: Binary Time Series, Dynamic Probit, Kalman Filter, Particle Filter, State-Space Model, Unified Skew-Normal.

1. Introduction

Despite the availability of several alternative approaches for dynamic inference and prediction of binary time series (MacDonald and Zucchini, 1997), state-space models provide a source of continuous interest due to their flexibility in accommodating a variety of representations and dependence structures via a tractable formulation (West and Harrison, 2006; Petris et al., 2009; Durbin and Koopman, 2012). Let $\mathbf{y}_t = (y_{1t}, \dots, y_{mt})^\top \in \{0, 1\}^m$ denote a vector of binary event data observed at time t , for $t = 1, \dots, n$, and define with $\boldsymbol{\theta}_t = (\theta_{1t}, \dots, \theta_{pt})^\top \in \mathbb{R}^p$ the corresponding vector of latent state variables. Adapting the notation in Petris et al. (2009) to our specific setting, we aim to provide closed-form expressions for the predictive and filtering distributions in the multivariate dynamic probit model defined as

$$p(\mathbf{y}_t | \boldsymbol{\theta}_t) = \Phi_m(\mathbf{B}_t \mathbf{F}_t \boldsymbol{\theta}_t; \mathbf{B}_t \mathbf{V}_t \mathbf{B}_t), \quad (1)$$

$$\boldsymbol{\theta}_t = \mathbf{G}_t \boldsymbol{\theta}_{t-1} + \boldsymbol{\varepsilon}_t, \quad \boldsymbol{\varepsilon}_t \sim N_p(\mathbf{0}, \mathbf{W}_t), \quad t = 1 \dots, n, \quad \boldsymbol{\theta}_0 \sim N_p(\mathbf{a}_0, \mathbf{P}_0), \quad (2)$$

where $\Phi_m(\mathbf{B}_t \mathbf{F}_t \boldsymbol{\theta}_t; \mathbf{B}_t \mathbf{V}_t \mathbf{B}_t)$ is the cumulative distribution function of the $N_m(\mathbf{0}, \mathbf{B}_t \mathbf{V}_t \mathbf{B}_t)$ evaluated at $\mathbf{B}_t \mathbf{F}_t \boldsymbol{\theta}_t$, with $\mathbf{B}_t = \text{diag}(2y_{1t} - 1, \dots, 2y_{mt} - 1)$ denoting the binary data matrix which characterizes the multivariate probit likelihood in (1). The quantities $\mathbf{F}_t, \mathbf{V}_t, \mathbf{G}_t, \mathbf{W}_t, \mathbf{a}_0$ and \mathbf{P}_0 define, instead, known matrices controlling the location, scale and dependence behavior of the state-space model (1)–(2). Although estimation and inference for these matrices is, itself, a relevant problem which can be addressed both from a frequentist and a Bayesian perspective, our focus in the present article is on providing exact results for dynamic inference on state variables and prediction of future binary events under model (1)–(2). Hence, consistent with the classical Kalman filter setting (Kalman, 1960), we rely on known system matrices $\mathbf{F}_t, \mathbf{V}_t, \mathbf{G}_t, \mathbf{W}_t, \mathbf{a}_0$ and \mathbf{P}_0 .

Model (1)–(2) defines a general representation encompassing a variety of formulations. For example, setting $\mathbf{V}_t = \mathbf{I}_m$ in (1) leads to a standard probit regression, for each $t = 1, \dots, n$, which includes also

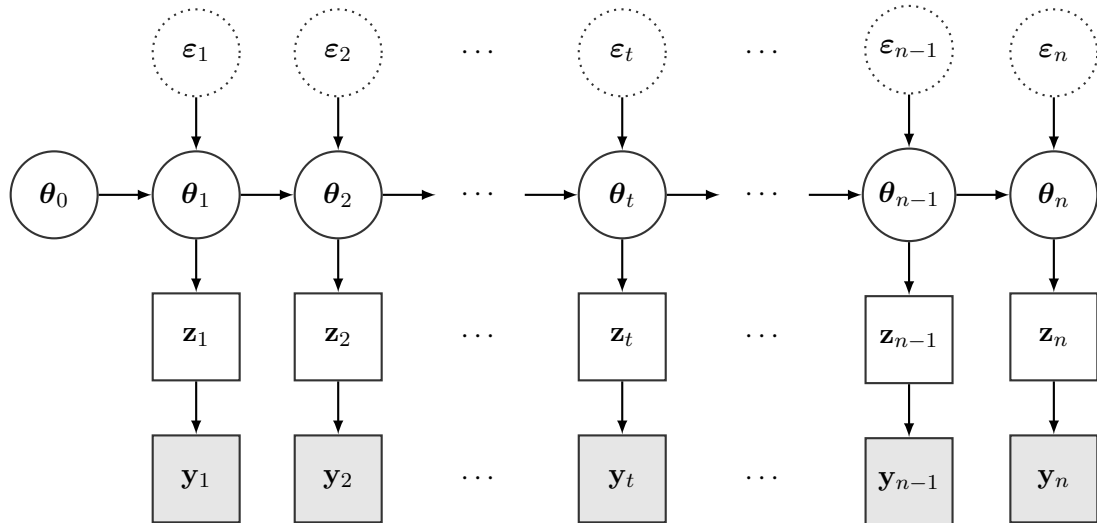


Fig. 1. Graphical representation of model (3)–(5). Dashed circles, solid circles, white squares and grey squares denote Gaussian errors, Gaussian states, latent Gaussian data and observed binary data, respectively.

the classical univariate dynamic probit model when $m = 1$. These representations have appeared in several applications, especially within the econometrics literature due to a direct connection between (1)–(2) and dynamic discrete choice models (Keane and Wolpin, 2009). Indeed, representation (1)–(2) can be alternatively obtained via the dichotomization of an underlying state-space model for the time series of m -variate Gaussian variables $\mathbf{z}_t = (z_{1t}, \dots, z_{mt})^\top \in \mathbb{R}^m$, $t = 1, \dots, n$, which can be regarded as unobserved time-varying utilities, from an econometric perspective. In particular, adapting classical results from probit regression (Albert and Chib, 1993), model (1)–(2), is equivalent to

$$\mathbf{y}_t = (y_{1t}, \dots, y_{mt})^\top = \mathbf{1}(\mathbf{z}_t > \mathbf{0}) = [1(z_{1t} > 0), \dots, 1(z_{mt} > 0)]^\top, \quad t = 1, \dots, n, \quad (3)$$

with $\mathbf{z}_1, \dots, \mathbf{z}_n$ evolving in time according to the Gaussian state-space model

$$p(\mathbf{z}_t | \boldsymbol{\theta}_t) = \phi_m(\mathbf{z}_t - \mathbf{F}_t \boldsymbol{\theta}_t; \mathbf{V}_t), \quad (4)$$

$$\boldsymbol{\theta}_t = \mathbf{G}_t \boldsymbol{\theta}_{t-1} + \boldsymbol{\varepsilon}_t, \quad \boldsymbol{\varepsilon}_t \sim N_p(\mathbf{0}, \mathbf{W}_t), \quad t = 1 \dots, n, \quad \boldsymbol{\theta}_0 \sim N_p(\mathbf{a}_0, \mathbf{P}_0), \quad (5)$$

having the usual dependence structure as expressed by the directed acyclic graph in Figure 1. In (4), $\phi_m(\mathbf{z}_t - \mathbf{F}_t \boldsymbol{\theta}_t; \mathbf{V}_t)$ denotes the Gaussian density for \mathbf{z}_t , with mean $\mathbf{F}_t \boldsymbol{\theta}_t$ and covariance matrix \mathbf{V}_t . To clarify the connection between (1)–(2) and (3)–(5), note that the generic element $y_{lt} = 1(z_{lt} > 0)$ of \mathbf{y}_t is either 1 or 0 depending on whether $z_{lt} > 0$ or $z_{lt} \leq 0$. Hence, with a slight abuse of notation, let us consider a generic vector $\mathbf{y}_t \in \{0; 1\}^m$ for which the probability mass function (1) is computed and denote with $\mathbf{B}_t = \text{diag}(2y_{1t} - 1, \dots, 2y_{mt} - 1)$ the associated $m \times m$ sign matrix. Then, one obtains $p(\mathbf{y}_t | \boldsymbol{\theta}_t) = \text{pr}(\mathbf{B}_t \mathbf{z}_t > \mathbf{0}) = \text{pr}[-\mathbf{B}_t(\mathbf{z}_t - \mathbf{F}_t \boldsymbol{\theta}_t) \leq \mathbf{B}_t \mathbf{F}_t \boldsymbol{\theta}_t] = \Phi_m(\mathbf{B}_t \mathbf{F}_t \boldsymbol{\theta}_t; \mathbf{B}_t \mathbf{V}_t \mathbf{B}_t)$, provided that $-\mathbf{B}_t(\mathbf{z}_t - \mathbf{F}_t \boldsymbol{\theta}_t) \sim N_m(\mathbf{0}, \mathbf{B}_t \mathbf{V}_t \mathbf{B}_t)$ under (4).

As is clear from (4)–(5), if $\mathbf{z}_{1:t} = (\mathbf{z}_1, \dots, \mathbf{z}_t)$ were observed, dynamic inference on the states $\boldsymbol{\theta}_t$, for $t = 1, \dots, n$, would be possible via direct application of the Kalman filter (Kalman, 1960). Indeed, exploiting Gaussian-Gaussian conjugacy and the conditional independence properties of state-space models, the predictive $p(\boldsymbol{\theta}_t | \mathbf{z}_{1:t-1})$ and filtering $p(\boldsymbol{\theta}_t | \mathbf{z}_{1:t})$ distributions are also Gaussian and have parameters which can be computed recursively via simple expressions relying on the previous updates. However, in (3)–(5), only a dichotomized version \mathbf{y}_t of \mathbf{z}_t is available, and hence the predictive and filtering distributions are $p(\boldsymbol{\theta}_t | \mathbf{y}_{1:t-1})$ and $p(\boldsymbol{\theta}_t | \mathbf{y}_{1:t})$, respectively. Recalling model (1)–(2) and Bayes rule, the calculation of these quantities proceeds by updating the Gaussian distribution for the states in (2) with the probit likelihood in (1), thereby providing conditional distributions which seem not available in closed form (Albert and Chib, 1993).

A common solution to the above issue is to rely on approximations of model (1)–(2) which allow the implementation of standard Kalman filter updates, thus leading to approximate dynamic inference on the state variables via extended (Uhlmann, 1992) or unscented (Julier and Uhlmann, 1997) Kalman filters, among others. However, as discussed by Andrieu and Doucet (2002), in many realistic studies these approximate methods could lead to unreliable inference. Markov Chain Monte Carlo strategies (Carlin et al., 1992; Carter and Kohn, 1994; Shephard, 1994; Song, 2000) address this issue, but, unlike the classical Kalman filter updates, these methods are not suitable for online prediction and filtering, thus facing computational bottlenecks. This has motivated an increasing interest in sequential Monte Carlo solutions (Doucet et al., 2001) providing particle-based representations of the conditional states distributions, which are then propagated in time to facilitate online dynamic inference (Gordon et al., 1993; Kitagawa, 1996; Liu and Chen, 1998; Pitt and Shephard, 1999; Doucet et al., 2000; Andrieu and Doucet, 2002). Although these strategies provide state-of-the-art methods for tractable prediction and filtering in non-Gaussian state-space models, sequential Monte Carlo is still sub-optimal compared to the case in which $p(\boldsymbol{\theta}_t | \mathbf{y}_{1:t-1})$ and $p(\boldsymbol{\theta}_t | \mathbf{y}_{1:t})$ are available in closed form and belong to a tractable class of distributions whose parameters can be sequentially updated in time via simple expressions.

In Section 3.1, we prove that, for the multivariate dynamic probit model in (1)–(2), the quantities $p(\boldsymbol{\theta}_t | \mathbf{y}_{1:t-1})$ and $p(\boldsymbol{\theta}_t | \mathbf{y}_{1:t})$ are unified skew-normal (SUN) distributions (Arellano-Valle and Azzalini, 2006) having tractable expressions for the recursive updating of the corresponding parameters. To the best of our knowledge, this novel result provides the first closed-form Kalman filter for dichotomous time series and allows for improvements in online dynamic inference within such a framework. Indeed, as highlighted in Section 2, SUN variables have several closure properties (Arellano-Valle and Azzalini, 2006; Azzalini and Capitanio, 2013) in addition to explicit formulas—involving cumulative distribution functions of multivariate normals—for the moments (Azzalini and Bacchieri, 2010; Gupta et al., 2013), and a tractable stochastic representation via a linear combination of Gaussian and truncated Gaussian variables, which facilitates sampling (Arellano-Valle and Azzalini, 2006; Azzalini and Capitanio, 2013). Also the normalizing constant is available (Arellano-Valle and Azzalini, 2006), thus providing a closed-form expression, derived in Section 3.1, for the predictive distribution $p(\mathbf{y}_t | \mathbf{y}_{1:t-1})$ of \mathbf{y}_t .

The above results improve sequential Monte Carlo by allowing online dynamic inference on filtering and predictive distributions via closed-form expressions, numerical evaluations or Monte Carlo integration based on independent samples from a SUN. As outlined in an illustrative study in Section 4.1, these strategies improve state-of-the-art methods. However, as discussed in Section 4, the multivariate Gaussian integrals entering the moments' expressions and the multivariate truncated Gaussians involved in sampling have a dimension which increases with t and m . Still, recent advances in dealing with these quantities (Botev, 2017) facilitate computationally efficient inference and sampling in small-to-moderate dimensional time series. In higher-dimensional settings, we propose instead a novel particle filter which exploits the SUN properties to obtain an optimal (Doucet et al., 2000) sequential Monte Carlo which effectively scales with t ; see Section 4.2. Future directions of research are discussed in Section 5. Finally, Appendix A completes our contribution by proving that also the smoothing distribution $p(\boldsymbol{\theta}_t | \mathbf{y}_{1:n})$ has a SUN kernel, under model (1)–(2).

2. The unified skew-normal distribution

Before deriving the SUN filtering and predictive distributions associated with model (1)–(2), let us first briefly review the SUN random variable. Arellano-Valle and Azzalini (2006) proposed this class to unify different generalizations (Arnold and Beaver, 2000; Arnold et al., 2002; Gupta et al., 2004; González-Farías et al., 2004) of the original multivariate skew-normal (Azzalini and Dalla Valle, 1996), whose density is obtained as the product of a multivariate Gaussian density and the cumulative distribution function of a standard normal evaluated at a value which depends on a skewness-inducing vector of

parameters. Motivated by the success of this formulation and of its various generalizations (Azzalini and Capitanio, 1999), Arellano-Valle and Azzalini (2006) developed a unifying representation, namely the unified skew-normal distribution. Under this class, a random vector $\boldsymbol{\theta}$ has a unified skew-normal distribution, $\boldsymbol{\theta} \sim \text{SUN}_{p,h}(\boldsymbol{\xi}, \boldsymbol{\Omega}, \boldsymbol{\Delta}, \boldsymbol{\gamma}, \boldsymbol{\Gamma})$, if its density function can be expressed as

$$p(\boldsymbol{\theta}) = \phi_p(\boldsymbol{\theta} - \boldsymbol{\xi}; \boldsymbol{\Omega}) \frac{\Phi_h[\boldsymbol{\gamma} + \boldsymbol{\Delta}^\top \bar{\boldsymbol{\Omega}}^{-1} \boldsymbol{\omega}^{-1}(\boldsymbol{\theta} - \boldsymbol{\xi}); \boldsymbol{\Gamma} - \boldsymbol{\Delta}^\top \bar{\boldsymbol{\Omega}}^{-1} \boldsymbol{\Delta}]}{\Phi_h(\boldsymbol{\gamma}; \boldsymbol{\Gamma})}, \quad (6)$$

where $\phi_p(\boldsymbol{\theta} - \boldsymbol{\xi}; \boldsymbol{\Omega})$ represents the density of a $N_p(\boldsymbol{\xi}, \boldsymbol{\Omega})$ whose covariance matrix $\boldsymbol{\Omega} = \boldsymbol{\omega} \bar{\boldsymbol{\Omega}} \boldsymbol{\omega}$ is obtained by re-scaling the correlation matrix $\bar{\boldsymbol{\Omega}}$ via the positive diagonal scale matrix $\boldsymbol{\omega} = (\boldsymbol{\Omega} \circ \mathbf{I}_p)^{1/2}$, with \circ denoting the element-wise Hadamard product. In (6), the skewness inducing mechanism is driven by the cumulative distribution function of the $N_h(\mathbf{0}, \boldsymbol{\Gamma} - \boldsymbol{\Delta}^\top \bar{\boldsymbol{\Omega}}^{-1} \boldsymbol{\Delta})$ computed at $\boldsymbol{\gamma} + \boldsymbol{\Delta}^\top \bar{\boldsymbol{\Omega}}^{-1} \boldsymbol{\omega}^{-1}(\boldsymbol{\theta} - \boldsymbol{\xi})$, whereas $\Phi_h(\boldsymbol{\gamma}; \boldsymbol{\Gamma})$ denotes the normalizing constant obtained by evaluating the cumulative distribution function of a $N_h(\mathbf{0}, \boldsymbol{\Gamma})$ at $\boldsymbol{\gamma}$. Arellano-Valle and Azzalini (2006) added a further identifiability condition which restricts the matrix $\boldsymbol{\Omega}^*$, having block entries $\boldsymbol{\Omega}_{[11]}^* = \boldsymbol{\Gamma}$, $\boldsymbol{\Omega}_{[22]}^* = \bar{\boldsymbol{\Omega}}$ and $\boldsymbol{\Omega}_{[21]}^* = \boldsymbol{\Omega}_{[12]}^{*\top} = \boldsymbol{\Delta}$, to be a full-rank correlation matrix.

To clarify the role of the parameters in equation (6), let us discuss a generative representation of the unified skew-normal which provides also basic intuitions on our results for the filtering and predictive distributions in model (1)–(2). In particular, letting $\mathbf{z}_0 \in \mathfrak{R}^h$ and $\boldsymbol{\theta}_0 \in \mathfrak{R}^p$ characterize two random vectors jointly distributed as a $N_{h+p}(\mathbf{0}, \boldsymbol{\Omega}^*)$, then $(\boldsymbol{\xi} + \boldsymbol{\omega} \boldsymbol{\theta}_0 \mid \mathbf{z}_0 + \boldsymbol{\gamma} > \mathbf{0}) \sim \text{SUN}_{p,h}(\boldsymbol{\xi}, \boldsymbol{\Omega}, \boldsymbol{\Delta}, \boldsymbol{\gamma}, \boldsymbol{\Gamma})$ (Arellano-Valle and Azzalini, 2006). Hence, $\boldsymbol{\xi}$ and $\boldsymbol{\omega}$ control location and scale, respectively, whereas the matrices $\boldsymbol{\Gamma}$, $\bar{\boldsymbol{\Omega}}$ and $\boldsymbol{\Delta}$ characterize the dependence structure within $\mathbf{z}_0 \in \mathfrak{R}^h$, $\boldsymbol{\theta}_0 \in \mathfrak{R}^p$ and between these two random vectors, respectively. Finally, $\boldsymbol{\gamma}$ controls the truncation mechanism in the partially observed Gaussian vector $\mathbf{z}_0 \in \mathfrak{R}^h$. Besides clarifying the meaning of the SUN parameters, such a result already provides initial key insights on our exact Kalman filter for the dynamic probit model (1)–(2). Indeed, according to (3)–(5), the filtering and predictive distributions induced by model (1)–(2) can be also defined as $p[\boldsymbol{\theta}_t \mid 1(\mathbf{z}_1 > \mathbf{0}), \dots, 1(\mathbf{z}_t > \mathbf{0})]$ and $p[\boldsymbol{\theta}_t \mid 1(\mathbf{z}_1 > \mathbf{0}), \dots, 1(\mathbf{z}_{t-1} > \mathbf{0})]$, respectively, with $(\mathbf{z}_t, \boldsymbol{\theta}_t)$ from the Gaussian state-space model (4)–(5) for $t = 1, \dots, n$, thus highlighting the direct connection between these distributions of interest and the generative representation of the SUN.

Another fundamental stochastic representation of the SUN distribution relies on linear combinations of Gaussian and truncated Gaussian random variables, thereby facilitating sampling from the SUN. In particular, recalling Azzalini and Capitanio (2013, Chapter 7.1.2) and Arellano-Valle and Azzalini (2006), if $\boldsymbol{\theta} \sim \text{SUN}_{p,h}(\boldsymbol{\xi}, \boldsymbol{\Omega}, \boldsymbol{\Delta}, \boldsymbol{\gamma}, \boldsymbol{\Gamma})$, then

$$\boldsymbol{\theta} \stackrel{d}{=} \boldsymbol{\xi} + \boldsymbol{\omega}(\mathbf{U}_0 + \boldsymbol{\Delta} \boldsymbol{\Gamma}^{-1} \mathbf{U}_1), \quad \mathbf{U}_0 \perp \mathbf{U}_1, \quad (7)$$

with $\mathbf{U}_0 \sim N_p(\mathbf{0}, \bar{\boldsymbol{\Omega}} - \boldsymbol{\Delta} \boldsymbol{\Gamma}^{-1} \boldsymbol{\Delta}^\top)$ and \mathbf{U}_1 from a $N_h(\mathbf{0}, \boldsymbol{\Gamma})$ truncated below $-\boldsymbol{\gamma}$. As we will clarify in Section 3, this result facilitates efficient Monte Carlo inference on complex functionals of the filtering and predictive distributions in model (1)–(2), based on sampling from the corresponding SUN variable. Indeed, although key moments can be explicitly derived via direct differentiation of the SUN moment generating function (Arellano-Valle and Azzalini, 2006; Gupta et al., 2013), such a strategy requires tedious calculations in the unified skew-normal framework, when the focus is on complex functionals. Moreover, recalling Azzalini and Bacchieri (2010) and Gupta et al. (2013), the first and second order moments further require the evaluation of h -variate Gaussian cumulative distribution functions $\Phi_h(\cdot)$, thus affecting computational tractability in large h settings (Botev, 2017). In these situations, Monte Carlo integration provides an effective solution, especially when independent samples can be generated. Therefore, we mostly focus on improved online Monte Carlo inference in model (1)–(2) exploiting the SUN properties, and refer to Azzalini and Bacchieri (2010) and Gupta et al. (2013) for a closed form expression of the expectation, variance and cumulative distribution function of SUN variables. Indeed, as clarified in Section 3, h increases linearly with time t in the SUN filtering and predictive distributions.

Before concluding our overview on SUNs, we shall emphasize that unified skew-normal variables are also closed under marginalization, linear combinations and conditioning (Arellano-Valle and Azzalini, 2006; Gupta et al., 2013; Azzalini and Capitanio, 2013). As clarified in Section 3, these key closure properties facilitate the derivation of the SUN filtering and predictive distributions in model (1)–(2).

3. Exact Kalman filter for binary time series

In this section we prove that exact Kalman filters—meant here as closed-form updating schemes for predictive and filtering distributions based on recursive expressions for the associated parameters—can be also derived for model (1)–(2). Section 3.1 derives in detail this novel filter, whereas Section 4 discusses the associated computational methods. Consistent with classical Kalman filters, we focus on predictive and filtering distributions. Similar results for smoothing can be found in Appendix A.

3.1. Exact Kalman filter updates

As a first step toward deriving the exact form of $p(\boldsymbol{\theta}_t | \mathbf{y}_{1:t-1})$ and $p(\boldsymbol{\theta}_t | \mathbf{y}_{1:t})$ under model (1)–(2), let us focus on $p(\boldsymbol{\theta}_1 | \mathbf{y}_1)$. This first filtering distribution characterizes the initial step of the Kalman filter recursion, and its expression provides key intuitions to obtain the state predictive $p(\boldsymbol{\theta}_t | \mathbf{y}_{1:t-1})$ and filtering $p(\boldsymbol{\theta}_t | \mathbf{y}_{1:t})$, for every $t \geq 2$. Lemma 1 states that $p(\boldsymbol{\theta}_1 | \mathbf{y}_1)$ is a SUN distribution. In the following, consistent with the notation of Section 2, whenever $\boldsymbol{\Omega}$ is a p -dimensional covariance matrix, the lower-case and the bar are used to denote $\boldsymbol{\omega} = (\boldsymbol{\Omega} \circ \mathbf{I}_p)^{1/2}$ and $\bar{\boldsymbol{\Omega}} = \boldsymbol{\omega}^{-1} \boldsymbol{\Omega} \boldsymbol{\omega}^{-1}$, respectively.

LEMMA 1. *Under the dynamic probit model (1)–(2), the initial filtering distribution is*

$$(\boldsymbol{\theta}_1 | \mathbf{y}_1) \sim \text{SUN}_{p,m}(\boldsymbol{\xi}_{1|1}, \boldsymbol{\Omega}_{1|1}, \boldsymbol{\Delta}_{1|1}, \gamma_{1|1}, \boldsymbol{\Gamma}_{1|1}), \quad (8)$$

with parameters $\boldsymbol{\xi}_{1|1} = \mathbf{G}_1 \mathbf{a}_0$, $\boldsymbol{\Omega}_{1|1} = \mathbf{G}_1 \mathbf{P}_0 \mathbf{G}_1^\top + \mathbf{W}_1$, $\boldsymbol{\Delta}_{1|1} = \bar{\boldsymbol{\Omega}}_{1|1} \boldsymbol{\omega}_{1|1} \mathbf{F}_1^\top \mathbf{B}_1 \mathbf{s}_1^{-1}$, $\gamma_{1|1} = \mathbf{s}_1^{-1} \mathbf{B}_1 \mathbf{F}_1 \boldsymbol{\xi}_{1|1}$ and $\boldsymbol{\Gamma}_{1|1} = \mathbf{s}_1^{-1} \mathbf{B}_1 (\mathbf{F}_1 \boldsymbol{\Omega}_{1|1} \mathbf{F}_1^\top + \mathbf{V}_1) \mathbf{B}_1 \mathbf{s}_1^{-1}$, where $\mathbf{s}_1 = [(\mathbf{F}_1 \boldsymbol{\Omega}_{1|1} \mathbf{F}_1^\top + \mathbf{V}_1) \circ \mathbf{I}_m]^{\frac{1}{2}}$.

Hence $p(\boldsymbol{\theta}_1 | \mathbf{y}_1)$ is a SUN distribution and its parameters can be obtained via tractable arithmetic expressions applied to the quantities characterizing model (1)–(2). The proof of Lemma 1, along with those of Theorem 1 and Corollary 1 presented below, can be found in Appendix B and expand recent conjugacy results for unified skew-normal priors in Bayesian probit models (Durante, 2019). Adapting these conjugacy properties and Lemma 1, the general Kalman filter updates for the multivariate probit model can be obtained by induction for $t \geq 2$ and are presented in Theorem 1.

THEOREM 1. *Let $(\boldsymbol{\theta}_{t-1} | \mathbf{y}_{1:t-1}) \sim \text{SUN}_{p,m,(t-1)}(\boldsymbol{\xi}_{t-1|t-1}, \boldsymbol{\Omega}_{t-1|t-1}, \boldsymbol{\Delta}_{t-1|t-1}, \gamma_{t-1|t-1}, \boldsymbol{\Gamma}_{t-1|t-1})$ be the filtering distribution at time $t-1$ in model (1)–(2). Then the predictive distribution is*

$$(\boldsymbol{\theta}_t | \mathbf{y}_{1:t-1}) \sim \text{SUN}_{p,m,(t-1)}(\boldsymbol{\xi}_{t|t-1}, \boldsymbol{\Omega}_{t|t-1}, \boldsymbol{\Delta}_{t|t-1}, \gamma_{t|t-1}, \boldsymbol{\Gamma}_{t|t-1}), \quad (9)$$

with parameters $\boldsymbol{\xi}_{t|t-1} = \mathbf{G}_t \boldsymbol{\xi}_{t-1|t-1}$, $\boldsymbol{\Omega}_{t|t-1} = \mathbf{G}_t \boldsymbol{\Omega}_{t-1|t-1} \mathbf{G}_t^\top + \mathbf{W}_t$, $\boldsymbol{\Delta}_{t|t-1} = \boldsymbol{\omega}_{t|t-1}^{-1} \mathbf{G}_t \boldsymbol{\omega}_{t-1|t-1} \boldsymbol{\Delta}_{t-1|t-1}$, $\gamma_{t|t-1} = \gamma_{t-1|t-1}$ and $\boldsymbol{\Gamma}_{t|t-1} = \boldsymbol{\Gamma}_{t-1|t-1}$. Moreover, the filtering distribution at time t is

$$(\boldsymbol{\theta}_t | \mathbf{y}_{1:t}) \sim \text{SUN}_{p,m,t}(\boldsymbol{\xi}_{t|t}, \boldsymbol{\Omega}_{t|t}, \boldsymbol{\Delta}_{t|t}, \gamma_{t|t}, \boldsymbol{\Gamma}_{t|t}), \quad (10)$$

with parameters $\boldsymbol{\xi}_{t|t} = \boldsymbol{\xi}_{t|t-1}$, $\boldsymbol{\Omega}_{t|t} = \boldsymbol{\Omega}_{t|t-1}$, $\boldsymbol{\Delta}_{t|t} = [\boldsymbol{\Delta}_{t|t-1}, \bar{\boldsymbol{\Omega}}_{t|t} \boldsymbol{\omega}_{t|t} \mathbf{F}_t^\top \mathbf{B}_t \mathbf{s}_t^{-1}]$, $\gamma_{t|t} = [\gamma_{t|t-1}, \boldsymbol{\xi}_{t|t}^\top \mathbf{F}_t^\top \mathbf{B}_t \mathbf{s}_t^{-1}]^\top$ and $\boldsymbol{\Gamma}_{t|t}$ a full-rank correlation matrix with blocks $\boldsymbol{\Gamma}_{t|t[11]} = \boldsymbol{\Gamma}_{t|t-1}$, $\boldsymbol{\Gamma}_{t|t[22]} = \mathbf{s}_t^{-1} \mathbf{B}_t (\mathbf{F}_t \boldsymbol{\Omega}_{t|t} \mathbf{F}_t^\top + \mathbf{V}_t) \mathbf{B}_t \mathbf{s}_t^{-1}$ and $\boldsymbol{\Gamma}_{t|t[21]} = \boldsymbol{\Gamma}_{t|t[12]}^\top = \mathbf{s}_t^{-1} \mathbf{B}_t \mathbf{F}_t \boldsymbol{\omega}_{t|t-1} \boldsymbol{\Delta}_{t|t-1}$, where $\mathbf{s}_t = [(\mathbf{F}_t \boldsymbol{\Omega}_{t|t} \mathbf{F}_t^\top + \mathbf{V}_t) \circ \mathbf{I}_m]^{\frac{1}{2}}$.

Consistent with Theorem 1, online prediction and filtering in the dynamic multivariate probit model (1)–(2) proceeds by iterating between equations (9) and (10) as new observations stream in with time t . Both steps are based on closed-form distributions and rely on analytical expressions for recursive

updating of the corresponding parameters as a function of the previous ones, thus providing the analog of the classical Kalman filter for Gaussian linear state-space models.

We also provide closed-form results for the predictive distribution of the multivariate binary data. Indeed, the prediction of future events $\mathbf{y}_t \in \{0; 1\}^m$ given the current data $\mathbf{y}_{1:t-1}$, is a primary goal in applications of dynamic probit models. Within our setting, this task requires the derivation of the predictive distribution $p(\mathbf{y}_t | \mathbf{y}_{1:t-1})$ which coincides with $\int \Phi_m(\mathbf{B}_t \mathbf{F}_t \boldsymbol{\theta}_t; \mathbf{B}_t \mathbf{V}_t \mathbf{B}_t) p(\boldsymbol{\theta}_t | \mathbf{y}_{1:t-1}) d\boldsymbol{\theta}_t$ under model (1)–(2), where $p(\boldsymbol{\theta}_t | \mathbf{y}_{1:t-1})$ is the state predictive distribution in (9). Corollary 1, shows that this quantity has an explicit form.

COROLLARY 1. *Under model (1)–(2), the observation predictive distribution $p(\mathbf{y}_t | \mathbf{y}_{1:t-1})$ is*

$$p(\mathbf{y}_t | \mathbf{y}_{1:t-1}) = \frac{\Phi_{m \cdot t}(\boldsymbol{\gamma}_{t|t}; \boldsymbol{\Gamma}_{t|t})}{\Phi_{m \cdot (t-1)}(\boldsymbol{\gamma}_{t|t-1}; \boldsymbol{\Gamma}_{t|t-1})}, \quad (11)$$

for every time t , with parameters $\boldsymbol{\gamma}_{t|t}$, $\boldsymbol{\Gamma}_{t|t}$, $\boldsymbol{\gamma}_{t|t-1}$ and $\boldsymbol{\Gamma}_{t|t-1}$, defined as in Theorem 1.

Hence, the evaluation of probabilities of future events is possible via explicit calculations after marginalizing out analytically the predictive distribution of the states. As is clear from (11), this approach requires the calculation of Gaussian cumulative distribution functions whose dimension increases with t and m . Efficient evaluation of these integrals is possible for small-to-moderate t and m via recent minimax tilting (Botev, 2017). However, these methods become impractical in large t and m studies. In Section 4, we develop novel Monte Carlo and sequential Monte Carlo strategies to overcome this issue and allow scalable inference exploiting results in Theorem 1 to improve current solutions.

4. Computational methods for dynamic inference

As discussed in Sections 2 and 3, inference without sampling from (9)–(10) is, theoretically, possible. Indeed, since the SUN densities of the predictive and filtering distributions are available from Theorem 1, the main functionals of interest can be computed either via closed-form expressions (Arellano-Valle and Azzalini, 2006; Azzalini and Bacchieri, 2010; Gupta et al., 2013; Azzalini and Capitanio, 2013) or by relying on numerical integration methods (e.g., Quarteroni et al., 2010). However, these strategies require multiple evaluations of multivariate Gaussian cumulative distribution functions and, hence, tend to be impractical as t increases or when the focus is on complex functionals.

Monte Carlo integration provides a tractable solution to these issues, if a computationally efficient strategy is available to sample independent and identically distributed values from (9)–(10). Exploiting the SUN properties and the results in Botev (2017), such a strategy is developed in Section 4.1 and is shown to improve state-of-the-art computational methods by avoiding issues of approximate inference and sequential Monte Carlo solutions, especially in small-to-moderate t settings. When t is large, a more scalable sequential Monte Carlo with optimality properties is also proposed in Section 4.2. The performance of these two algorithms is quantitatively evaluated on two real-data illustrative applications in Sections 4.1.1 and 4.2.1, respectively.

4.1. Monte Carlo methods

Monte Carlo methods allow accurate evaluation of generic functionals $E[g(\boldsymbol{\theta}_t) | \mathbf{y}_{1:t}]$ and $E[g(\boldsymbol{\theta}_{t+1}) | \mathbf{y}_{1:t}]$ for the filtering and predictive distribution via

$$\frac{1}{R} \sum_{r=1}^R g(\boldsymbol{\theta}_{t|t}^{(r)}) \quad \text{and} \quad \frac{1}{R} \sum_{r=1}^R g(\boldsymbol{\theta}_{t+1|t}^{(r)}), \quad \text{for } t = 1, \dots, n,$$

where $\boldsymbol{\theta}_{t|t}^{(1)}, \dots, \boldsymbol{\theta}_{t|t}^{(R)}$ and $\boldsymbol{\theta}_{t+1|t}^{(1)}, \dots, \boldsymbol{\theta}_{t+1|t}^{(R)}$ are samples from $p(\boldsymbol{\theta}_t | \mathbf{y}_{1:t})$ and $p(\boldsymbol{\theta}_{t+1} | \mathbf{y}_{1:t})$, respectively. For example, the observation predictive distribution $p(\mathbf{y}_t | \mathbf{y}_{1:t-1})$ can be alternatively computed as $\sum_{r=1}^R \Phi_m(\mathbf{B}_t \mathbf{F}_t \boldsymbol{\theta}_{t|t-1}^{(r)}; \mathbf{B}_t \mathbf{V}_t \mathbf{B}_t) / R$ if the evaluation of (11) is computationally demanding.

Algorithm 1: Exact scheme to draw independent samples from $p(\boldsymbol{\theta}_t \mid \mathbf{y}_{1:t})$, for $t = 1, \dots, n$

```

for  $t$  from 1 to  $n$  do
  [1] Sample  $\mathbf{U}_{0\ t|t}^{(1)}, \dots, \mathbf{U}_{0\ t|t}^{(R)}$  independently from a  $N_p(\mathbf{0}, \bar{\boldsymbol{\Omega}}_{t|t} - \boldsymbol{\Delta}_{t|t} \boldsymbol{\Gamma}_{t|t}^{-1} \boldsymbol{\Delta}_{t|t}^\top)$ .
  [2] Sample  $\mathbf{U}_{1\ t|t}^{(1)}, \dots, \mathbf{U}_{1\ t|t}^{(R)}$  independently from a  $N_{m \cdot t}(\mathbf{0}, \boldsymbol{\Gamma}_{t|t})$  truncated below  $-\gamma_{t|t}$ 
  [3] Compute  $\boldsymbol{\theta}_{t|t}^{(1)}, \dots, \boldsymbol{\theta}_{t|t}^{(R)}$  via  $\boldsymbol{\theta}_{t|t}^{(r)} = \boldsymbol{\xi}_{t|t} + \boldsymbol{\omega}_{t|t}(\mathbf{U}_{0\ t|t}^{(r)} + \boldsymbol{\Delta}_{t|t} \boldsymbol{\Gamma}_{t|t}^{-1} \mathbf{U}_{1\ t|t}^{(r)})$  for each  $r = 1, \dots, R$ 

```

Although the above samples can be obtained via Markov Chain Monte Carlo or sequential Monte Carlo methods, the optimal solution, if possible, is to rely on independent and identically distributed (i.i.d.) realizations from $p(\boldsymbol{\theta}_t \mid \mathbf{y}_{1:t})$ and $p(\boldsymbol{\theta}_{t+1} \mid \mathbf{y}_{1:t})$. Leveraging our exact Kalman filter in Section 3 and the additive representation (7) of the unified skew-normal, independent realizations $\boldsymbol{\theta}_{t|t}^{(1)}, \dots, \boldsymbol{\theta}_{t|t}^{(R)}$ from the filtering distribution in (10) can be obtained via a linear combination between independent samples from p -variate Gaussians and $m \cdot t$ -variate truncated normals. Algorithm 1 provides a pseudo-code for this novel routine, whose outputs are i.i.d. samples from the filtering distribution, for every $t = 1, \dots, n$. The most computationally intensive step is the sampling from the multivariate truncated normals. In fact, although efficient Hamiltonian Monte Carlo solutions are available (Pakman and Paninski, 2014), these strategies do not provide independent samples. More recently, an accept-reject method based on minimax tilting has been proposed by Botev (2017) to improve the acceptance rate of classical rejection sampling, while avoiding convergence and mixing issues of MCMC. Such a routine is available in the R library `TruncatedNormal` and allows efficient sampling from multivariate truncated normals having a dimension of few hundreds, thereby providing effective Monte Carlo inference via Algorithm 1 in small-to-moderate dimensional time series. In this setting such a routine can be seen as online, in practice, since i.i.d. samples from the exact filtering are simulated rapidly, for each t .

Based on realizations $\boldsymbol{\theta}_{t|t}^{(1)}, \dots, \boldsymbol{\theta}_{t|t}^{(R)}$ from the filtering distribution in equation (10), i.i.d. samples from the predictive distribution can be simply generated via direct application of equation (2) to obtain $\boldsymbol{\theta}_{t+1|t}^{(1)} = \mathbf{G}_{t+1} \boldsymbol{\theta}_{t|t}^{(1)} + \boldsymbol{\varepsilon}_{t+1}^{(1)}, \dots, \boldsymbol{\theta}_{t+1|t}^{(R)} = \mathbf{G}_{t+1} \boldsymbol{\theta}_{t|t}^{(R)} + \boldsymbol{\varepsilon}_{t+1}^{(R)}$, for each time $t = 1, \dots, n$, with $\boldsymbol{\varepsilon}_{t+1}^{(1)}, \dots, \boldsymbol{\varepsilon}_{t+1}^{(R)}$ denoting independent samples from $N_p(\mathbf{0}, \mathbf{W}_{t+1})$. Hence, efficient Monte Carlo inference in small-to-moderate dimensional dynamic probit models is possible also for the predictive distribution.

4.1.1. Application to small-to-moderate time series

We evaluate the performance of Algorithm 1 in an illustrative univariate time series measuring the annual outcome of the Oxford–Cambridge boat race from 1946 to 2018 (Durbin and Koopman, 2012). In this study, each y_t is either 1 or 0 if the winner is Cambridge or Oxford, respectively, at time $t = 1, \dots, 73$, and the main focus is on providing dynamic inference and prediction for such a binary time series. In accomplishing this goal, Durbin and Koopman (2012) consider a random walk formulation for the state equation, which leads to the dynamic probit model

$$\begin{aligned}
 p(y_t \mid \theta_t) &= \Phi[(2y_t - 1)\theta_t; 1], \\
 \theta_t &= \theta_{t-1} + \varepsilon_t, \quad \varepsilon_t \sim N(0, W_t), \quad t = 1 \dots, 73, \quad \theta_0 \sim N(a_0, P_0).
 \end{aligned} \tag{12}$$

Although more complex state-space models and higher-dimensional time series could be considered, this setting is not uncommon in several studies. Moreover, our main goal in this study is to evaluate the performance of the sampling strategy defined in Algorithm 1, using the exact filtering distribution (10) computed on a finite grid as a benchmark. Hence, consistent with this aim, we consider an application where the exact calculation of the filtering density is possible, in practice, for any $t = 1, \dots, n$.

To clarify the improvements provided by Algorithm 1, we further compare its performance with the relevant competing strategies mentioned in Section 1. These methods include the extended Kalman filter (Uhlmann, 1992), the bootstrap particle filter (Gordon et al., 1993) and the Rao-Blackwellized sequential Monte Carlo by Andrieu and Doucet (2002) which leverages the hierarchical representation

Table 1. For different numbers of particles R , Wasserstein distance (averaged across time and 100 replicated experiments) between the empirical filtering distribution induced by the particles generated under each sampling method and the one obtained by direct evaluation of the exact density (10) on a grid of 7000 equally spaced values in $[-7, 7]$.

	$R = 100$	$R = 200$	$R = 500$	$R = 1000$
Exact SUN Monte Carlo Sampler	0.12712	0.09018	0.05769	0.04127
Rao-Blackwellized Particle Filter	0.19360	0.13707	0.08845	0.06256
Bootstrap Particle Filter	0.22766	0.16419	0.10480	0.07450
Extended Kalman Filter	0.31207	0.29567	0.28589	0.28178

(3)–(5) of model (1)–(2). Although being a popular solution in routine implementations, the extended Kalman filter relies on a quadratic approximation of the probit log-likelihood which leads to a Gaussian filtering distribution, thereby affecting quality of online learning. The bootstrap particle filter (Gordon et al., 1993) is, instead, motivated by the apparent absence of a tractable optimal proposal distribution $p(\boldsymbol{\theta}_t | \boldsymbol{\theta}_{t-1|t-1}^{(r)}, \mathbf{y}_t)$ (Doucet et al., 2000) and, therefore, proposes values from $p(\boldsymbol{\theta}_t | \boldsymbol{\theta}_{t-1|t-1}^{(r)})$. Also Rao-Blackwellized sequential Monte Carlo (Andrieu and Doucet, 2002) aims at providing an alternative particle filter, which addresses the apparent unavailability of an analytical expression for the optimal proposal and the corresponding importance weights. The authors overcome this key issue by proposing a sequential Monte Carlo strategy for the Rao-Blackwellized filtering distribution $p(\mathbf{z}_t | \mathbf{y}_{1:t})$ of the partially observed Gaussian data \mathbf{z}_t in model (3)–(5) and compute, for each particle’s trajectory $\mathbf{z}_{1:t}^{(r)}$, relevant moments of $p(\boldsymbol{\theta}_t | \mathbf{z}_{1:t}^{(r)})$ via classical Kalman filter updates—applied to model (4)–(5)—which are then averaged across the particles to obtain a Monte Carlo estimate for the moments of $p(\boldsymbol{\theta}_t | \mathbf{y}_{1:t})$.

Although the above methods provide state-of-the-art solutions, the proposed strategies are motivated by the apparent absence of an exact Kalman filter for model (1)–(2), which is actually available according to our results in Section 3. Table 1 highlights to what extent such a novel finding improves the existing methods for online inference under model (1)–(2). More specifically, Table 1 compares the Wasserstein distances (e.g. Villani, 2008), averaged both across time and 100 replicated experiments, between the empirical filtering distribution induced by the particles generated from each sampling method under analysis and the one obtained by direct evaluation of the exact density (10) on a grid of 7000 equally spaced values in $[-7, 7]$. Such a distance is computed via the R function `wasserstein1d` for an increasing number of particles R , with $W_t = 0.5$, $a_0 = 0$ and $P_0 = 5$ to obtain similar settings as in Durbin and Koopman (2012). Although the extended Kalman filter and the Rao-Blackwellized sequential Monte Carlo focus, mostly, on the first two central moments of $p(\boldsymbol{\theta}_t | \mathbf{y}_{1:t})$, these strategies can be naturally adapted to draw samples from an approximation of the filtering distribution. For the sake of clarity, the term *particle* is used to denote both the samples of the sequential Monte Carlo methods and those obtained under i.i.d. sampling via Algorithm 1.

Table 1 confirms that a higher number of particles R leads to a natural improvement for all the sampling schemes, with the proposed exact sampler in Algorithm 1 over-performing all the competitors for every R , as expected. Such a result is due to the fact that the extended Kalman filter relies on an approximation of the filtering distribution, whereas, unlike the proposed exact sampler, the bootstrap and the Rao-Blackwellized particle filters consider sub-optimal dependent sampling strategies. Not surprisingly, the Rao-Blackwellized particle filter is the second best choice. Nonetheless, as expected, exact i.i.d. sampling from the SUN filtering distribution via Algorithm 1 remains the optimal solution and provides a viable strategy which is essentially online in any small-to-moderate time series study.

4.2. Optimal particle filter

When the dimension of the dynamic probit model (1)–(2) increases, sampling from multivariate truncated Gaussians in Algorithm 1 can face computational bottlenecks (Botev, 2017). This is particularly likely to occur in series monitored on a fine time grid. Indeed, in several applications, the number of

Algorithm 2: Optimal particle filter to draw approximate samples from $p(\boldsymbol{\theta}_t | \mathbf{y}_{1:t})$, for $t=1, \dots, n$

for t from 1 to n do

 for r from 1 to R do

- [1] Propose a value $\bar{\boldsymbol{\theta}}_{t|t}^{(r)}$ by sampling from (13) conditioned on $\boldsymbol{\theta}_{t-1} = \boldsymbol{\theta}_{t-1|t-1}^{(r)}$. In particular
 - [1.1] Sample $\mathbf{U}_{0\ t|t}^{(r)}$ from a $N_p(\mathbf{0}, \bar{\boldsymbol{\Omega}}_{t|t,t-1} - \boldsymbol{\Delta}_{t|t,t-1} \boldsymbol{\Gamma}_{t|t,t-1}^{-1} \boldsymbol{\Delta}_{t|t,t-1}^\top)$.
 - [1.2] Sample $\mathbf{U}_{1\ t|t}^{(r)}$ from a $N_m(\mathbf{0}, \boldsymbol{\Gamma}_{t|t,t-1})$ truncated below $-\boldsymbol{\gamma}_{t|t,t-1}^{(r)} = -\mathbf{c}_t^{-1} \mathbf{B}_t \mathbf{F}_t \mathbf{G}_t \boldsymbol{\theta}_{t-1|t-1}^{(r)}$.
 - [1.3] Compute $\bar{\boldsymbol{\theta}}_{t|t}^{(r)} = \boldsymbol{\xi}_{t|t,t-1}^{(r)} + \boldsymbol{\omega}_{t|t,t-1} (\mathbf{U}_{0\ t|t}^{(r)} + \boldsymbol{\Delta}_{t|t,t-1} \boldsymbol{\Gamma}_{t|t,t-1}^{-1} \mathbf{U}_{1\ t|t}^{(r)})$, with $\boldsymbol{\xi}_{t|t,t-1}^{(r)} = \mathbf{G}_t \boldsymbol{\theta}_{t-1|t-1}^{(r)}$.
 - [2] Calculate the associated importance weight $w_t^{(r)}$ exploiting (14) and normalize them.
 - [3] Obtain $\boldsymbol{\theta}_{t|t}^{(1)}, \dots, \boldsymbol{\theta}_{t|t}^{(R)}$ by resampling from $\bar{\boldsymbol{\theta}}_{t|t}^{(1)}, \dots, \bar{\boldsymbol{\theta}}_{t|t}^{(R)}$ with weights $w_t^{(1)}, \dots, w_t^{(R)}$.
-

time series m is small-to-moderate, whereas the length of the time window can be particularly large. To address this issue and allow scalable online inference also in large t settings, we propose a particle filter which exploits the SUN results to obtain optimality properties.

The proposed algorithm belongs to the class of sequential importance sampling-resampling (SISR) algorithms which provide default strategies in particle filtering (e.g., Doucet et al., 2000, 2001; Durbin and Koopman, 2012). For each time t , these routines sample R trajectories $\boldsymbol{\theta}_{1:t|t}^{(1)}, \dots, \boldsymbol{\theta}_{1:t|t}^{(R)}$, known as *particles*, conditioned on those produced at $t-1$, by iterating, in time, between the two steps below.

Importance sampling. Let $\boldsymbol{\theta}_{1:t-1|t-1}^{(1)}, \dots, \boldsymbol{\theta}_{1:t-1|t-1}^{(R)}$ be the particles produced at time $t-1$ and denote with $\pi(\boldsymbol{\theta}_{t|t} | \boldsymbol{\theta}_{1:t-1}, \mathbf{y}_{1:t})$ the selected proposal. Then, for each $r = 1, \dots, R$,

- (i) Sample $\bar{\boldsymbol{\theta}}_{t|t}^{(r)}$ from $\pi(\boldsymbol{\theta}_{t|t} | \boldsymbol{\theta}_{1:t-1|t-1}^{(r)}, \mathbf{y}_{1:t})$ and set $\bar{\boldsymbol{\theta}}_{t|t}^{(r)} = (\boldsymbol{\theta}_{1:t-1|t-1}^{(r)\top}, \bar{\boldsymbol{\theta}}_{t|t}^{(r)\top})^\top$.
- (ii) Compute the weights $w_t^{(r)} = w_t(\bar{\boldsymbol{\theta}}_{1:t|t}^{(r)}) \propto p(\mathbf{y}_t | \bar{\boldsymbol{\theta}}_{t|t}^{(r)}) p(\bar{\boldsymbol{\theta}}_{t|t}^{(r)} | \boldsymbol{\theta}_{t-1|t-1}^{(r)}) \pi(\bar{\boldsymbol{\theta}}_{t|t}^{(r)} | \boldsymbol{\theta}_{1:t-1|t-1}^{(r)}, \mathbf{y}_{1:t})^{-1}$ and normalize them to ensure that their sum is 1.

Resampling. For $r = 1, \dots, R$, sample the new particles $\boldsymbol{\theta}_{1:t|t}^{(1)}, \dots, \boldsymbol{\theta}_{1:t|t}^{(R)}$ from $\sum_{l=1}^R w_t^{(l)} \delta_{\bar{\boldsymbol{\theta}}_{1:t|t}^{(l)}}$.

Based on these particles, inference on the filtering distribution $p(\boldsymbol{\theta}_t | \mathbf{y}_{1:t})$ can proceed by exploiting the terminal values $\boldsymbol{\theta}_{t|t}^{(1)}, \dots, \boldsymbol{\theta}_{t|t}^{(R)}$ of each trajectory $\boldsymbol{\theta}_{1:t|t}^{(1)}, \dots, \boldsymbol{\theta}_{1:t|t}^{(R)}$.

As is clear from the above steps, the performance of SISR relies on the proposal $\pi(\boldsymbol{\theta}_{t|t} | \boldsymbol{\theta}_{1:t-1}, \mathbf{y}_{1:t})$. This importance function should allow tractable sampling along with efficient evaluation of the importance weights, and should be also carefully specified to propose effective candidate samples. Recalling Doucet et al. (2000), the optimal importance density is $\pi(\boldsymbol{\theta}_{t|t} | \boldsymbol{\theta}_{1:t-1}, \mathbf{y}_{1:t}) = p(\boldsymbol{\theta}_t | \boldsymbol{\theta}_{t-1}, \mathbf{y}_t)$ with weights $w_t(\boldsymbol{\theta}_{1:t}) \propto p(\mathbf{y}_t | \boldsymbol{\theta}_{t-1})$. Indeed, this choice minimizes the variance of the importance weights, thereby limiting degeneracy issues and improving mixing. Unfortunately, in several dynamic models, tractable sampling from $p(\boldsymbol{\theta}_t | \boldsymbol{\theta}_{t-1}, \mathbf{y}_t)$ and direct calculation of $p(\mathbf{y}_t | \boldsymbol{\theta}_{t-1})$ is typically not possible (e.g. Doucet et al., 2000). As outlined in Corollary 2, this is not the case for multivariate dynamic probit models. In particular, as a direct consequence of Theorem 1 and of the closure properties of the SUN, sampling from $p(\boldsymbol{\theta}_t | \boldsymbol{\theta}_{t-1}, \mathbf{y}_t)$ is straightforward and $p(\mathbf{y}_t | \boldsymbol{\theta}_{t-1})$ can be efficiently evaluated.

COROLLARY 2. Under the dynamic model (1)–(2), the following results hold for each $t = 1, \dots, n$.

$$(\boldsymbol{\theta}_t | \boldsymbol{\theta}_{t-1}, \mathbf{y}_t) \sim \text{SUN}_{p,m}(\boldsymbol{\xi}_{t|t,t-1}, \boldsymbol{\Omega}_{t|t,t-1}, \boldsymbol{\Delta}_{t|t,t-1}, \boldsymbol{\gamma}_{t|t,t-1}, \boldsymbol{\Gamma}_{t|t,t-1}), \quad (13)$$

$$p(\mathbf{y}_t | \boldsymbol{\theta}_{t-1}) = \Phi_m(\boldsymbol{\gamma}_{t|t,t-1}; \boldsymbol{\Gamma}_{t|t,t-1}), \quad (14)$$

with $\boldsymbol{\xi}_{t|t,t-1} = \mathbf{G}_t \boldsymbol{\theta}_{t-1}$, $\boldsymbol{\Omega}_{t|t,t-1} = \mathbf{W}_t$, $\boldsymbol{\Delta}_{t|t,t-1} = \bar{\boldsymbol{\Omega}}_{t|t,t-1} \boldsymbol{\omega}_{t|t,t-1} \mathbf{F}_t^\top \mathbf{B}_t \mathbf{c}_t^{-1}$, $\boldsymbol{\gamma}_{t|t,t-1} = \mathbf{c}_t^{-1} \mathbf{B}_t \mathbf{F}_t \boldsymbol{\xi}_{t|t,t-1}$, $\boldsymbol{\Gamma}_{t|t,t-1} = \mathbf{c}_t^{-1} \mathbf{B}_t (\mathbf{F}_t \boldsymbol{\Omega}_{t|t,t-1} \mathbf{F}_t^\top + \mathbf{V}_t) \mathbf{B}_t \mathbf{c}_t^{-1}$, where $\mathbf{c}_t = [(\mathbf{F}_t \boldsymbol{\Omega}_{t|t,t-1} \mathbf{F}_t^\top + \mathbf{V}_t) \circ \mathbf{I}_m]^{1/2}$.

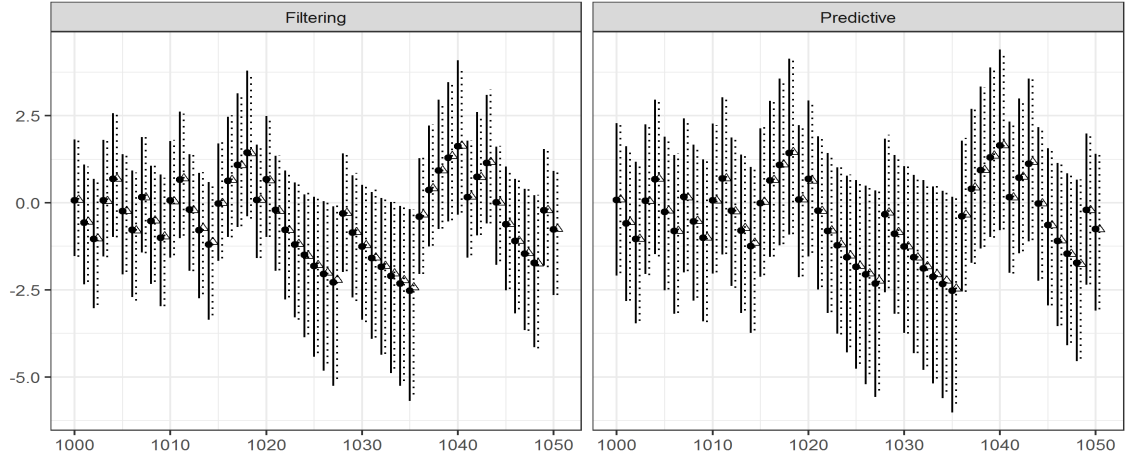


Fig. 2. Comparison between the optimal particle filter from Algorithm 2 and the Rao-Blackwellized one. Circles and continuous segments represent the median and the 90% credible intervals for the predictive and filtering distributions based on 10^4 samples from the Rao-Blackwellized particle filter. Triangles and dotted segments denote the same quantities computed from 10^4 particles produced by the optimal particle filter.

Algorithm 2 illustrates the pseudo-code of the proposed optimal filter, which exploits the additive representation of the SUN and Corollary 2. Comparing Algorithms 1 and 2 it can be noticed that now the computational complexity of the different steps does not depend on t , thereby facilitating scalable sequential inference in large t studies. Samples from the predictive distribution can be obtained from those of the filtering as discussed in Section 4.1.

4.2.1. Application to large time series

In this section the performance of Algorithm 2 is evaluated on the illustrative time series of monthly rainfalls in Bungaree, Australia, from January 1882 to December 2018, having $n = 1640$ time-indexed observations. Data are available at the Australian Government website and our focus is on the binary series with values $y_t = 1$ if the rainfalls in month t exceed 70 millimeters and 0 otherwise. For the purpose of this study, we assume again model (12) and consider the same settings of Section 4.1.1.

We compare the samples produced by the particle filter in Algorithm 2 with those generated by the Rao-Blackwellized sequential Monte Carlo routine, which has been shown to provide a scalable and accurate strategy in Section 4.1.1. In this application we consider 10^4 samples for both algorithms to evaluate performance under a number of particles that would be considered in practice. Figure 2 outlines the medians and 90% credible intervals of the state filtering and predictive distributions obtained from the particles under each method, for the period $t = 1000, \dots, 1050$ to improve readability. As it can be noticed, the results are equivalent. The similarity of the two outputs is not a specific feature of the selected time window. In fact, the time-averaged Wasserstein distance between the state filtering and predictive distributions produced by the two particle filters are 0.030 and 0.029, respectively. Also the computational time of the two routines was essentially equal. These results confirm the accuracy of our novel particle filter and provide further support to the Rao-Blackwellized algorithm. We shall, however, emphasize that Algorithm 2 has a formal constructive motivation directly tied to the exact Kalman filter in Section 3 and avoids data augmentations.

5. Discussion

This article shows that the filtering and predictive distributions in a dynamic probit model for multivariate binary time series have a SUN kernel and the associated parameters can be updated online via

tractable expressions. As discussed in Section 3, such a novel exact Kalman filter provides advances in online inference for dynamic binary data and facilitates the implementation of tractable methods to draw independent and identically distributed samples from the exact filtering and predictive distributions, thus allowing improved Monte Carlo inference in small-to-moderate time series studies. High-dimensional filtering can be, instead, implemented via a scalable sequential Monte Carlo method which exploits SUN properties to provide a particle filter based on optimal proposals.

These results motivate additional future research. For instance, a relevant direction is to adapt or generalize the derivations in Section 3 to dynamic tobit and binomial or multinomial probit models, for which exact Kalman filters are unavailable. Joint filtering and prediction of continuous and binary time series is also of key interest (Liu et al., 2009). A natural state-space model for these multivariate data can be obtained by generalizing (3)–(5) to allow only the subset of Gaussian variables associated with the binary data to be partially observed. However, also in this case, closed form Kalman filters are not available. By combining our results in Section 3 with the classical Kalman filter for Gaussian state-space models, such a gap could be possibly covered. As discussed in Section 1, estimation and inference for possible unknown parameters characterizing the state-space model in (1)–(2) is another interesting problem which can be addressed adapting frequentist (Gupta and Aziz, 2012) and Bayesian methods (Canale and Scarpa, 2016) for SUN variables. Finally, additional quantitative studies beyond those in Section 4 can be useful in obtaining a more comprehensive overview on the performance of our proposed computational methods compared to state-of-the-art strategies.

Appendix A: Smoothing distribution

To obtain the smoothing equations we first prove that $p(\boldsymbol{\theta}_{1:n} | \mathbf{y}_{1:n})$ is a unified skew-normal density, and then derive the classical smoothing distribution $p(\boldsymbol{\theta}_t | \mathbf{y}_{1:n})$ by exploiting the closure properties of the SUN under marginalization (Azzalini and Capitanio, 2013, Chapter 7.1.2). To accomplish this goal, first notice that $p(\boldsymbol{\theta}_{1:n} | \mathbf{y}_{1:n}) \propto p(\boldsymbol{\theta}_{1:n})p(\mathbf{y}_{1:n} | \boldsymbol{\theta}_{1:n})$. Hence, $p(\boldsymbol{\theta}_{1:n} | \mathbf{y}_{1:n})$ can be interpreted as the posterior distribution in the Bayesian model having likelihood $p(\mathbf{y}_{1:n} | \boldsymbol{\theta}_{1:n})$ and prior $p(\boldsymbol{\theta}_{1:n})$ for the $(p \cdot n) \times 1$ vector $\boldsymbol{\theta}_{1:n} = (\boldsymbol{\theta}_1^\top, \dots, \boldsymbol{\theta}_n^\top)^\top$.

Consistent with (2) and letting $\mathbf{G}_q^t = \mathbf{G}_t \cdots \mathbf{G}_q$, it can be easily proved that $p(\boldsymbol{\theta}_{1:n})$ is a Gaussian distribution having a $(p \cdot n) \times 1$ mean vector $\boldsymbol{\xi}$ with blocks $\boldsymbol{\xi}_{[t]} = \mathbb{E}(\boldsymbol{\theta}_t) = \mathbf{G}_1^t \mathbf{a}_0 \in \mathbb{R}^p$ for every time $t = 1, \dots, n$. Also the $(p \cdot n) \times (p \cdot n)$ covariance matrix $\boldsymbol{\Omega}$ has a block structure with $\boldsymbol{\Omega}_{[t,t]} = \text{var}(\boldsymbol{\theta}_t) = \mathbf{G}_1^t \mathbf{P}_0 \mathbf{G}_1^{t\top} + \sum_{q=2}^t \mathbf{G}_q^t \mathbf{W}_{q-1} \mathbf{G}_q^{t\top} + \mathbf{W}_t$, for $t = 1, \dots, n$, and $\boldsymbol{\Omega}_{[t,q]} = \boldsymbol{\Omega}_{[q,t]}^\top = \text{cov}(\boldsymbol{\theta}_t, \boldsymbol{\theta}_q) = \mathbf{G}_{q+1}^t \boldsymbol{\Omega}_{[q,q]}$, for $t > q$. The form of $p(\mathbf{y}_{1:n} | \boldsymbol{\theta}_{1:n})$ can be instead obtained from (1), by noticing that given $\boldsymbol{\theta}_{1:n}$ the vectors $\mathbf{y}_1, \dots, \mathbf{y}_n$ are conditionally independent, thus providing the joint likelihood $p(\mathbf{y}_{1:n} | \boldsymbol{\theta}_{1:n}) = \prod_{t=1}^n \Phi_m(\mathbf{B}_t \mathbf{F}_t \boldsymbol{\theta}_t; \mathbf{B}_t \mathbf{V}_t \mathbf{B}_t)$. Such a quantity can be also expressed as $\Phi_{m \cdot n}(\mathbf{D} \boldsymbol{\theta}_{1:n}; \mathbf{V})$ where \mathbf{D} and \mathbf{V} are $(m \cdot n) \times (p \cdot n)$ and $(m \cdot n) \times (m \cdot n)$ block-diagonal matrices with blocks $\mathbf{D}_{[t,t]} = \mathbf{B}_t \mathbf{F}_t \in \mathbb{R}^{m \times p}$ and $\mathbf{V}_{[t,t]} = \mathbf{B}_t \mathbf{V}_t \mathbf{B}_t \in \mathbb{R}^{m \times m}$, respectively, for every $t = 1, \dots, n$. Combining these results, the joint smoothing distribution $p(\boldsymbol{\theta}_{1:n} | \mathbf{y}_{1:n})$ is proportional to the kernel $\phi_{p \cdot n}(\boldsymbol{\theta}_{1:n} - \boldsymbol{\xi}; \boldsymbol{\Omega}) \Phi_{m \cdot n}(\mathbf{D} \boldsymbol{\theta}_{1:n}; \mathbf{V})$ of the unified skew-normal variable

$$(\boldsymbol{\theta}_{1:n} | \mathbf{y}_{1:n}) \sim \text{SUN}_{p \cdot n, m \cdot n}(\boldsymbol{\xi}_{1:n|n}, \boldsymbol{\Omega}_{1:n|n}, \boldsymbol{\Delta}_{1:n|n}, \boldsymbol{\gamma}_{1:n|n}, \boldsymbol{\Gamma}_{1:n|n}) \quad (15)$$

with $\boldsymbol{\xi}_{1:n|n} = \boldsymbol{\xi}$, $\boldsymbol{\Omega}_{1:n|n} = \boldsymbol{\Omega}$, $\boldsymbol{\Delta}_{1:n|n} = \bar{\boldsymbol{\Omega}} \boldsymbol{\omega} \mathbf{D}^\top \mathbf{s}^{-1}$, $\boldsymbol{\gamma}_{1:n|n} = \mathbf{s}^{-1} \mathbf{D} \boldsymbol{\xi}$, $\boldsymbol{\Gamma}_{1:n|n} = \mathbf{s}^{-1} (\mathbf{D} \boldsymbol{\Omega} \mathbf{D}^\top + \mathbf{V}) \mathbf{s}^{-1}$ and $\mathbf{s} = [(\mathbf{D} \boldsymbol{\Omega} \mathbf{D}^\top + \mathbf{V}) \circ \mathbf{I}_{m \cdot n}]^{1/2}$. Finally, since the SUN is closed under marginalization (Azzalini and Capitanio, 2013, Chapter 7.1.2), the smoothing distribution $p(\boldsymbol{\theta}_t | \mathbf{y}_{1:n})$ can be directly obtained from (15), for every $t = 1, \dots, n$, and coincides with

$$(\boldsymbol{\theta}_t | \mathbf{y}_{1:n}) \sim \text{SUN}_{p, m \cdot n}(\boldsymbol{\xi}_{t|n}, \boldsymbol{\Omega}_{t|n}, \boldsymbol{\Delta}_{t|n}, \boldsymbol{\gamma}_{t|n}, \boldsymbol{\Gamma}_{t|n}), \quad (16)$$

where $\boldsymbol{\xi}_{t|n} = \boldsymbol{\xi}_{[t]}$, $\boldsymbol{\Omega}_{t|n} = \boldsymbol{\Omega}_{[t,t]}$, $\boldsymbol{\gamma}_{t|n} = \boldsymbol{\gamma}_{1:n|n}$, $\boldsymbol{\Gamma}_{t|n} = \boldsymbol{\Gamma}_{1:n|n}$ and $\boldsymbol{\Delta}_{t|n} = \boldsymbol{\Delta}_{1:n|n[t]}$ denotes the t -th block of p rows in $\boldsymbol{\Delta}_{1:n|n}$.

Appendix B: Proofs of the main results

B.1. Proof of Lemma 1

To prove Lemma 1, it suffices to note that $p(\boldsymbol{\theta}_1 | \mathbf{y}_1)$ is the posterior in a Bayesian probit regression with likelihood $p(\mathbf{y}_1 | \boldsymbol{\theta}_1) = \Phi_m(\mathbf{B}_1 \mathbf{F}_1 \boldsymbol{\theta}_1; \mathbf{B}_1 \mathbf{V}_1 \mathbf{B}_1)$ and prior $p(\boldsymbol{\theta}_1) = \phi_p(\boldsymbol{\theta}_1 - \mathbf{G}_1 \mathbf{a}_0; \mathbf{G}_1 \mathbf{P}_0 \mathbf{G}_1^\top + \mathbf{W}_1)$, where the expression for $p(\boldsymbol{\theta}_1)$ can be easily obtained after noticing that $\boldsymbol{\theta}_1 = \mathbf{G}_1 \boldsymbol{\theta}_0 + \boldsymbol{\varepsilon}_1$ in (2), with $\boldsymbol{\theta}_0 \sim N_p(\mathbf{a}_0, \mathbf{P}_0)$ and $\boldsymbol{\varepsilon}_1 \sim N_p(\mathbf{0}, \mathbf{W}_1)$. Hence, Lemma 1 can be obtained from Theorem 1 in Durante (2019), replacing the identity matrix \mathbf{I}_m in the classical probit likelihood with $\mathbf{B}_1 \mathbf{V}_1 \mathbf{B}_1$. \square

B.2. Proof of Theorem 1

Recalling expression (2), the proof for $p(\boldsymbol{\theta}_t | \mathbf{y}_{1:t-1})$ in (9) requires studying the variable $\mathbf{G}_t \boldsymbol{\theta}_{t-1} + \boldsymbol{\varepsilon}_t$, given $\mathbf{y}_{1:t-1}$, where $(\boldsymbol{\theta}_{t-1} | \mathbf{y}_{1:t-1}) \sim \text{SUN}_{p,m,(t-1)}(\boldsymbol{\xi}_{t-1|t-1}, \boldsymbol{\Omega}_{t-1|t-1}, \boldsymbol{\Delta}_{t-1|t-1}, \boldsymbol{\gamma}_{t-1|t-1}, \boldsymbol{\Gamma}_{t-1|t-1})$ and $\boldsymbol{\varepsilon}_t \sim N_p(\mathbf{0}, \mathbf{W}_t)$, with $\boldsymbol{\varepsilon}_t \perp \mathbf{y}_{1:t-1}$. To address this goal, first note that, by the closure properties of the unified skew-normal under linear transformations (Azzalini and Capitanio, 2013, Chapter 7.1.2), the variable $(\mathbf{G}_t \boldsymbol{\theta}_{t-1} | \mathbf{y}_{1:t-1})$ is still a unified skew-normal and has parameters $\mathbf{G}_t \boldsymbol{\xi}_{t-1|t-1}$, $\mathbf{G}_t \boldsymbol{\Omega}_{t-1|t-1} \mathbf{G}_t^\top$, $[(\mathbf{G}_t \boldsymbol{\Omega}_{t-1|t-1} \mathbf{G}_t^\top) \circ \mathbf{I}_p]^{-1/2} \mathbf{G}_t \boldsymbol{\omega}_{t-1|t-1} \boldsymbol{\Delta}_{t-1|t-1}$, $\boldsymbol{\gamma}_{t-1|t-1}$ and $\boldsymbol{\Gamma}_{t-1|t-1}$. Hence, to conclude the proof of equation (9), we only need to obtain the distribution of the sum among this variable and the noise $\boldsymbol{\varepsilon}_t \sim N_p(\mathbf{0}, \mathbf{W}_t)$. This can be accomplished by considering the moment generating function of such a sum—as done by Azzalini and Capitanio (2013, Chapter 7.1.2) to prove closure under convolution. Indeed, it is straightforward to notice that the product of the moment generating functions for $\boldsymbol{\varepsilon}_t$ and $(\mathbf{G}_t \boldsymbol{\theta}_{t-1} | \mathbf{y}_{1:t-1})$ leads to the moment generating function of the unified skew-normal variable having parameters $\boldsymbol{\xi}_{t|t-1} = \mathbf{G}_t \boldsymbol{\xi}_{t-1|t-1}$, $\boldsymbol{\Omega}_{t|t-1} = \mathbf{G}_t \boldsymbol{\Omega}_{t-1|t-1} \mathbf{G}_t^\top + \mathbf{W}_t$, $\boldsymbol{\Delta}_{t|t-1} = \boldsymbol{\omega}_{t|t-1}^{-1} \mathbf{G}_t \boldsymbol{\omega}_{t-1|t-1} \boldsymbol{\Delta}_{t-1|t-1}$, $\boldsymbol{\gamma}_{t|t-1} = \boldsymbol{\gamma}_{t-1|t-1}$ and $\boldsymbol{\Gamma}_{t|t-1} = \boldsymbol{\Gamma}_{t-1|t-1}$.

To prove equation (10) it is, instead, sufficient to note that $p(\boldsymbol{\theta}_t | \mathbf{y}_{1:t}) \propto \Phi_m(\mathbf{B}_t \mathbf{F}_t \boldsymbol{\theta}_t; \mathbf{B}_t \mathbf{V}_t \mathbf{B}_t) p(\boldsymbol{\theta}_t | \mathbf{y}_{1:t-1})$, thus coinciding with the posterior in a probit regression having likelihood $\Phi_m(\mathbf{B}_t \mathbf{F}_t \boldsymbol{\theta}_t; \mathbf{B}_t \mathbf{V}_t \mathbf{B}_t)$ and SUN prior $p(\boldsymbol{\theta}_t | \mathbf{y}_{1:t-1})$ from (9). Hence, expression (10) can be derived from Corollary 4 in Durante (2019), replacing the matrix \mathbf{I}_m in the classical probit likelihood with $\mathbf{B}_t \mathbf{V}_t \mathbf{B}_t$. \square

B.3. Proof of Corollary 1

To prove Corollary 1, first notice that $\int \Phi_m(\mathbf{B}_t \mathbf{F}_t \boldsymbol{\theta}_t; \mathbf{B}_t \mathbf{V}_t \mathbf{B}_t) p(\boldsymbol{\theta}_t | \mathbf{y}_{1:t-1}) d\boldsymbol{\theta}_t$ can be also re-written as $\Phi_{m,(t-1)}(\boldsymbol{\gamma}_{t|t-1}; \boldsymbol{\Gamma}_{t|t-1})^{-1} \int \Phi_m(\mathbf{B}_t \mathbf{F}_t \boldsymbol{\theta}_t; \mathbf{B}_t \mathbf{V}_t \mathbf{B}_t) K(\boldsymbol{\theta}_t | \mathbf{y}_{1:t-1}) d\boldsymbol{\theta}_t$ where $K(\boldsymbol{\theta}_t | \mathbf{y}_{1:t-1}) = p(\boldsymbol{\theta}_t | \mathbf{y}_{1:t-1}) \Phi_{m,(t-1)}(\boldsymbol{\gamma}_{t|t-1}; \boldsymbol{\Gamma}_{t|t-1})$ is the kernel of the predictive distribution in equation (9). Consistent with this expression, Corollary 1 follows after noticing that $\Phi_m(\mathbf{B}_t \mathbf{F}_t \boldsymbol{\theta}_t; \mathbf{B}_t \mathbf{V}_t \mathbf{B}_t) K(\boldsymbol{\theta}_t | \mathbf{y}_{1:t-1})$ is the kernel of the filtering distribution in (10), whose normalizing constant $\int \Phi_m(\mathbf{B}_t \mathbf{F}_t \boldsymbol{\theta}_t; \mathbf{B}_t \mathbf{V}_t \mathbf{B}_t) K(\boldsymbol{\theta}_t | \mathbf{y}_{1:t-1}) d\boldsymbol{\theta}_t$ is equal to $\Phi_m(\boldsymbol{\gamma}_{t|t}; \boldsymbol{\Gamma}_{t|t})$. \square

B.4. Proof of Corollary 2

The proof of Corollary 2 is similar to the one of Lemma 1. Indeed, the proposal $p(\boldsymbol{\theta}_t | \boldsymbol{\theta}_{t-1}, \mathbf{y}_t)$ is the posterior in a Bayesian probit regression with likelihood $p(\mathbf{y}_t | \boldsymbol{\theta}_t) = \Phi_m(\mathbf{B}_t \mathbf{F}_t \boldsymbol{\theta}_t; \mathbf{B}_t \mathbf{V}_t \mathbf{B}_t)$ and prior $p(\boldsymbol{\theta}_t | \boldsymbol{\theta}_{t-1}) = \phi_p(\boldsymbol{\theta}_t - \mathbf{G}_t \boldsymbol{\theta}_{t-1}; \mathbf{W}_t)$. To derive the expression for the importance weights defined in equation (14), it is sufficient to notice that the marginal likelihood $p(\mathbf{y}_t | \boldsymbol{\theta}_{t-1})$ coincides with the normalizing constant of the SUN in equation (13). \square

References

Albert, J. H. and Chib, S. (1993) Bayesian analysis of binary and polychotomous response data. *Journal of the American Statistical Association*, **88**, 669–679.

- Andrieu, C. and Doucet, A. (2002) Particle filtering for partially observed Gaussian state space models. *Journal of the Royal Statistical Society: Series B (Statistical Methodology)*, **64**, 827–836.
- Arellano-Valle, R. B. and Azzalini, A. (2006) On the unification of families of skew-normal distributions. *Scandinavian Journal of Statistics*, **33**, 561–574.
- Arnold, B. C. and Beaver, R. J. (2000) Hidden truncation models. *Sankhyā: The Indian Journal of Statistics, Series A*, **62**, 23–35.
- Arnold, B. C., Beaver, R. J., Azzalini, A., Balakrishnan, N., Bhaumik, A., Dey, D., Cuadras, C. and Sarabia, J. M. (2002) Skewed multivariate models related to hidden truncation and/or selective reporting. *Test*, **11**, 7–54.
- Azzalini, A. and Bacchieri, A. (2010) A prospective combination of phase II and phase III in drug development. *Metron*, **68**, 347–369.
- Azzalini, A. and Capitanio, A. (1999) Statistical applications of the multivariate skew normal distribution. *Journal of the Royal Statistical Society: Series B (Statistical Methodology)*, **61**, 579–602.
- (2013) *The Skew-normal and Related Families*. Cambridge University Press.
- Azzalini, A. and Dalla Valle, A. (1996) The multivariate skew-normal distribution. *Biometrika*, **83**, 715–726.
- Botev, Z. (2017) The normal law under linear restrictions: simulation and estimation via minimax tilting. *Journal of the Royal Statistical Society: Series B (Statistical Methodology)*, **79**, 125–148.
- Canale, A. and Scarpa, B. (2016) Bayesian nonparametric location–scale–shape mixtures. *Test*, **25**, 113–130.
- Carlin, B. P., Polson, N. G. and Stoffer, D. S. (1992) A Monte Carlo approach to non-normal and nonlinear state-space modeling. *Journal of the American Statistical Association*, **87**, 493–500.
- Carter, C. K. and Kohn, R. (1994) On Gibbs sampling for state space models. *Biometrika*, **81**, 541–553.
- Doucet, A., De Freitas, N. and Gordon, N. (2001) *Sequential Monte Carlo Methods in Practice*. Springer.
- Doucet, A., Godsill, S. and Andrieu, C. (2000) On sequential Monte Carlo sampling methods for Bayesian filtering. *Statistics and Computing*, **10**, 197–208.
- Durante, D. (2019) Conjugate Bayes for probit regression via unified skew-normals. *Biometrika*, In press.
- Durbin, J. and Koopman, S. J. (2012) *Time Series Analysis by State Space Methods*. Oxford University Press.
- González-Farías, G., Dominguez-Molina, A. and Gupta, A. K. (2004) Additive properties of skew normal random vectors. *Journal of Statistical Planning and Inference*, **126**, 521–534.
- Gordon, N. J., Salmond, D. J. and Smith, A. F. (1993) Novel approach to nonlinear/non-Gaussian Bayesian state estimation. *IEE Proceedings F-radar and Signal Processing*, **140**, 107–113.
- Gupta, A. K. and Aziz, M. A. (2012) Estimation of parameters of the unified skew normal distribution using the method of weighted moments. *Journal of Statistical Theory and Practice*, **6**, 402–416.
- Gupta, A. K., Aziz, M. A. and Ning, W. (2013) On some properties of the unified skew-normal distribution. *Journal of Statistical Theory and Practice*, **7**, 480–495.

- Gupta, A. K., González-Farías, G. and Dominguez-Molina, J. A. (2004) A multivariate skew normal distribution. *Journal of Multivariate Analysis*, **89**, 181–190.
- Julier, S. J. and Uhlmann, J. K. (1997) New extension of the Kalman filter to nonlinear systems. In *Proceedings SPIE 3068, Signal Processing, Sensor Fusion, and Target Recognition*, 182–194.
- Kalman, R. E. (1960) A new approach to linear filtering and prediction problems. *Journal of Basic Engineering*, **82**, 35–45.
- Keane, M. P. and Wolpin, K. I. (2009) Empirical applications of discrete choice dynamic programming models. *Review of Economic Dynamics*, **12**, 1–22.
- Kitagawa, G. (1996) Monte Carlo filter and smoother for non-Gaussian nonlinear state space models. *Journal of Computational and Graphical Statistics*, **5**, 1–25.
- Liu, J. S. and Chen, R. (1998) Sequential Monte Carlo methods for dynamic systems. *Journal of the American Statistical Association*, **93**, 1032–1044.
- Liu, X., Daniels, M. J. and Marcus, B. (2009) Joint models for the association of longitudinal binary and continuous processes with application to a smoking cessation trial. *Journal of the American Statistical Association*, **104**, 429–438.
- MacDonald, I. L. and Zucchini, W. (1997) *Hidden Markov and Other Models for Discrete-Valued Time Series*. CRC Press.
- Pakman, A. and Paninski, L. (2014) Exact Hamiltonian Monte Carlo for truncated multivariate Gaussians. *Journal of Computational and Graphical Statistics*, **23**, 518–542.
- Petris, G., Petrone, S. and Campagnoli, P. (2009) *Dynamic Linear Models with R*. Springer.
- Pitt, M. K. and Shephard, N. (1999) Filtering via simulation: Auxiliary particle filters. *Journal of the American Statistical Association*, **94**, 590–599.
- Quarteroni, A., Sacco, R. and Saleri, F. (2010) *Numerical Mathematics (Second Edition)*. Springer Science & Business Media.
- Shephard, N. (1994) Partial non-Gaussian state space. *Biometrika*, **81**, 115–131.
- Song, P. X.-K. (2000) Monte Carlo Kalman filter and smoothing for multivariate discrete state space models. *Canadian Journal of Statistics*, **28**, 641–652.
- Uhlmann, J. K. (1992) Algorithms for multiple-target tracking. *American Scientist*, **80**, 128–141.
- Villani, C. (2008) *Optimal Transport: Old and New*. Springer Science & Business Media.
- West, M. and Harrison, J. (2006) *Bayesian Forecasting and Dynamic Models*. Springer Science & Business Media.